

A critical ligamentous mechanism in the evolution of avian flight

David B. Baier¹, Stephen M. Gatesy¹ & Farish A. Jenkins Jr²

Despite recent advances in aerodynamic^{1,2}, neuromuscular^{3–5} and kinematic^{6,7} aspects of avian flight and dozens of relevant fossil discoveries⁸, the origin of aerial locomotion and the transition from limbs to wings continue to be debated^{9,10}. Interpreting this transition depends on understanding the mechanical interplay of forces in living birds, particularly at the shoulder where most wing motion takes place. Shoulder function depends on a balance of forces from muscles, ligaments and articular cartilages, as well as inertial, gravitational and aerodynamic loads on the wing¹¹. Here we show that the force balance system of the shoulder evolved from a primarily muscular mechanism to one in which the acrocoracohumeral ligament has a critical role. Features of the shoulder of Mesozoic birds and closely related theropod dinosaurs indicate that the evolution of flight preceded the acquisition of the ligament-based force balance system and that some basal birds are intermediate in shoulder morphology.

Steady-speed gliding, in comparison to flapping, is more amenable to estimating the interplay of forces stabilizing the shoulder in flight. The minimum forces needed to hold the wing outstretched in a gliding pigeon are provided by a mathematical model¹². Each wing produces a vertical aerodynamic force at its centre of pressure¹³ of approximately 0.5BW (0.5 × body weight; Fig. 1a, b). This force engenders a moment about the shoulder (tending to elevate the wing relative to the body) that is countered by a downward force from the pectoralis muscle. The pectoralis acts with such a short lever arm (L_p , Fig. 1b) that a force of 7BW is required to balance the aerodynamic moment.

However, this model¹² inaccurately represents the shoulder as a sturdy ball-and-socket joint capable of fully supporting the wing. In reality, a large, ovoid humeral head articulates with a relatively shallow, saddle-shaped glenoid with open dorsal and ventral margins¹⁴ (Fig. 1c). The glenoid is structurally incapable of resisting the downward pull on the humerus as the pectoralis counters the elevation moment. Antagonistic muscles and/or ligaments must provide an upward force to preclude ventral dislocation.

The primary upstroke muscle, the supracoracoideus, might be expected to pull upward on the humerus, but its tendon actually pulls ventromedially (rotating the wing by an elevation/supination moment¹⁵ rather than by raising the humeral head). Only three of the twelve muscles crossing the shoulder are oriented to produce an upward force (scapulohumeralis, latissimus dorsi and the subcoracoscapulares complex; Table 1, $F_{y\max}$) in gliding. The acrocoracohumeral ligament (AHL, Fig. 1c), spanning from the acrocoracoid process of the coracoid to the transverse sulcus of the humerus, is also situated to preclude ventral dislocation. The ligament was predicted to limit wing pronation (in pigeon¹⁶), or constrain the normal range of flapping movements (in starling¹⁴). In swimming penguins, the AHL was inferred to be taut in all wing positions, effectively coordi-

nating shoulder movement and preventing disarticulation¹⁷. To explore the relative contributions of these four structures to joint stability, we undertook a force balance analysis of a wing in a gliding posture.

Three-dimensional force balance calculations that include the AHL yield a family of viable solutions in which all forces and moments equilibrate, requiring ligament forces of about 6–9BW and only small inputs from other muscles (Table 1; Fig. 2a, b). No combination of the three upward-pulling muscles can balance the system without the AHL. Higher forces (about 13BW) are generated by the pectoralis during flapping¹⁸, implying even greater demands on the AHL. Mechanical testing of the pigeon AHL reveals that the ligament can withstand tensile loading of 39BW ($\pm 5BW$, $n = 10$) without failure, far exceeding potential flight-induced forces. Following transection of the AHL, stimulation of the pectoralis or manipulation of the humerus in fresh specimens produces ventral shoulder dislocation, as expected. We conclude that the AHL is critical to maintaining the integrity of the shoulder joint during aerial locomotion. Rather than being supported from below by articular cartilage, the humeral head is suspended from above by the AHL.

The avian coracoid is typically described as a compressive strut between the wing and the sternum^{12,13} that resists loads generated by the pectoralis. Although the pectoralis vector generally aligns with the long axis of the coracoid, the laterally facing glenoid cannot by itself transmit a force from the humeral head down the coracoid's shaft. At the glenoid, our force balance predicts that the coracoid bears a medially directed load equal and opposite to the laterally directed joint force on the humeral head (F_j ; Fig. 2a, b). If unopposed, this force would push the coracoids together, compressing the thorax. The medial push on the glenoid is primarily balanced by the lateral pull of the AHL. The acrocoracoid process experiences a ventrolateral force equal and opposite to the dorsomedially directed AHL force experienced by the proximal humerus (F_{ahj} ; Fig. 2a, b). Compression at the glenoid and tension on the acrocoracoid process sum to a net ventromedial force that approximately aligns with the shaft of the coracoid. This net force can be primarily opposed by a dorsolateral force from the sternum at the coracosternal joint. The AHL thus provides a mechanism for transmitting the pectoralis force through the coracoid as a compressive strut.

Has AHL function evolved as a specialization for flight in birds or is its role primitive for archosaurs? Crocodylians, the closest extant relatives of birds, possess a homologous coracohumeral ligament (CHL) and, like birds, retain the ancestral archosaurian saddle-shaped glenoid¹⁴. However, in alligators, as in most other diapsids, the long axis of the glenoid is oriented approximately 90° to that of birds, such that the open margins of the joint are anterior and posterior (Fig. 2c). The alligator's humerus is supported ventrally by the coracoid portion of the glenoid saddle, but during locomotion

¹Department of Ecology and Evolutionary Biology, Brown University, Providence, Rhode Island 02912, USA. ²Department of Organismic and Evolutionary Biology and Museum of Comparative Zoology, Harvard University, Cambridge, Massachusetts 02138, USA.

Table 1 | Force magnitudes and force balance solutions

	F_{\max}	$F_{y\max}$	S1	S2	S3	S4
M. pectoralis	22.4	-19.7	5.9	5.1	6.1	6.0
M. supracoracoideus	10.2	-3.8	0	0	0	0
M. deltoideus, pars minor	1.1	-0.4	0	0	0.3	0.6
M. deltoideus, pars major	0.7	-0.1	0	0	0	0.4
M. scapulohumeralis	5.5	3.2	1.2	0	1.2	0.8
M. coracobrachialis cranialis	0.7	-0.2	0	0	0.3	0
M. coracobrachialis caudalis	3.1	-2.1	0	0	0	0
M. latissimus dorsi	0.5	0.2	0	0	0	0
M. biceps brachii	4.0	-0.6	0.2	0.2	0	0
M. scapulothriceps	4.5	-0.4	0	0	0	0
M. subcoracoscapulares	6.0	2.9	0	2.2	0	0.8
M. deltoideus, pars propatagialis	2.7	-0.3	0.5	0.6	0	0
Lig. acrocoracohumerale	39.0	20.7	8	6.0	8.5	8.1
Joint contact force	-	-	8.5	8.5	8.8	9.5
Total muscle force	-	-	7.8	8.1	7.9	8.6

Maximum force (F_{\max}) for muscles and ligaments crossing the shoulder joint of a pigeon was derived from physiological cross sectional area measurements, mechanical testing and published data. Maximum vertical force ($F_{y\max}$) is only upward (positive, bold) for three muscles and the AHL. Columns S1–S4 are four of the many possible 3D force balance solutions for gliding (details in Methods). All values are in multiples of body weight.

retractors such as the caudal part of the pectoralis pull the humeral head towards the open, posterior margin.

Unlike birds, crocodylians possess several muscles that arise from a broad scapulocoracoid plate anterior to the glenoid (Fig. 3a) and are thus capable of countering the pectoralis. Three-dimensional kin-

ematic records of the shoulder girdle and humerus of alligators walking on the treadmill were compared with ligament-taut positions derived from manipulating dissections. Minimal overlap between ligament-taut and walking humeral positions demonstrates that the CHL is slack throughout the majority of the stride cycle and therefore not essential for joint stabilization during locomotion. Electromyographic data from varanid lizards¹⁹ show that several muscles, despite their protractive lines of action, are active while the limb is retracting, suggesting a stabilizing role. Homologous protractor muscles in *Alligator mississippiensis* are also likely to be primarily responsible for balancing the pectoralis. We propose that shoulder joint stabilization evolved within archosaurs from a primarily active, muscle-based balance system to a passive, ligament-based system in extant, volant birds.

On the basis of comparative coracoid morphology in *Deinonychus*, *Archaeopteryx* and extant birds, the coracoid tuberosity of theropod dinosaurs is considered to be homologous with the avian acrocoracoid process²⁰. With reference to the tuberosity/process and other anatomical landmarks, we reconstructed the orientation of the scapulocoracoid and CHL/AHL for the non-avian theropods *Sinornithoides youngi* and *Sinornithosaurus millenii* and for the volant avialans *Archaeopteryx lithographica* and *Confuciusornis sanctus* (Fig. 3b–e). The ancestral ligament orientation of the CHL is retained in all but *C. sanctus* (Fig. 3e), in which elevation of the acrocoracoid process above the glenoid and deepening of the humeral head yield an

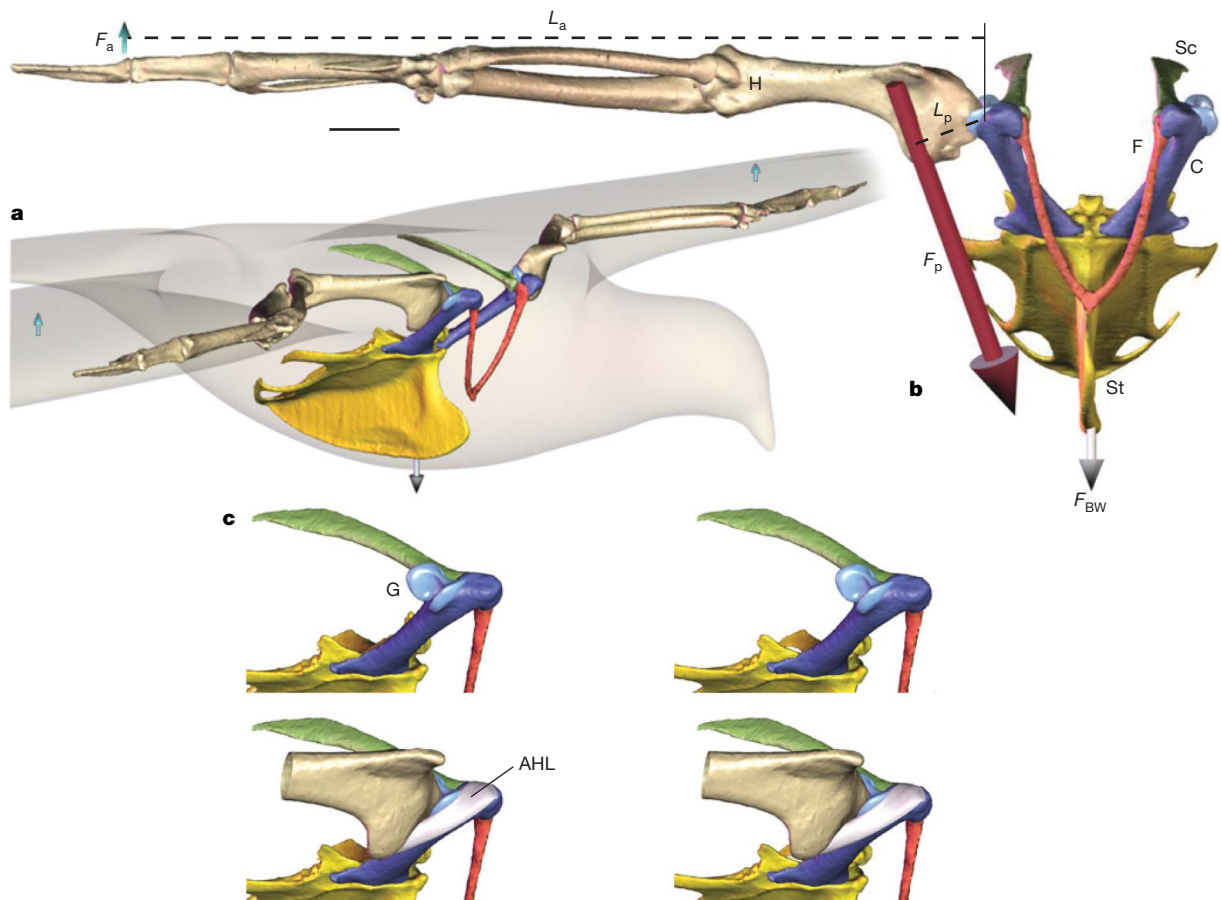


Figure 1 | Forelimb skeleton and pectoral girdle of a pigeon. **a, b**, Anterolateral (**a**) and anterior (**b**) views. During a steady speed glide the bird's body weight (downward grey vector shown below the chest, F_{BW}) is supported by aerodynamic forces of 0.5BW from each wing (upward blue vectors, F_a). F_a has a lever arm (L_a) about the shoulder approximately $11\times$ that of the pectoralis (L_p) requiring a pectoralis force (red vector, F_p) of about 6BW to balance the elevation moment. **c**, Anterolateral stereo pairs showing the saddle shaped glenoid (light blue, G), which lacks a ventral shelf to support the humeral head. The acrocoracohumeral ligament (AHL), spanning from the elevated acrocoracoid process of the coracoid to the transverse sulcus on the proximal humerus, is ideally situated to prevent ventral dislocation by the pectoralis. H, humerus, Sc, scapula (green), C, coracoid (blue), F, furcula (red), St, sternum (yellow). Scale bar in **b** equals 1 cm.

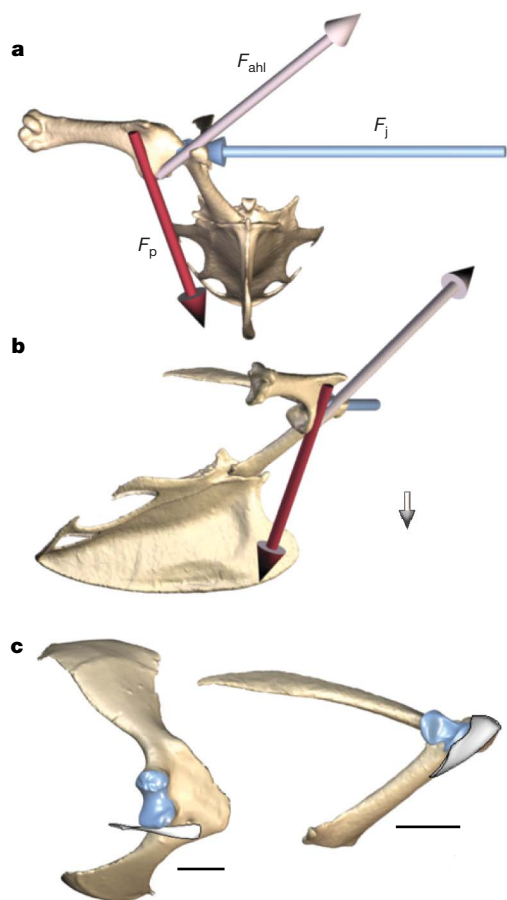


Figure 2 | Force balance for the glenohumeral joint of a gliding pigeon and comparison of alligator and pigeon shoulder morphology. **a, b**, Anterior (**a**) and right lateral (**b**) views of primary forces balancing the shoulder (S1, Table 1). The ventromedial force of the pectoralis (F_p) is resisted by the dorsomedial pull of the acrocoracohumeral ligament (F_{ahl}) and a lateral push from the glenoid (F_j). Aerodynamic and smaller muscle forces are not shown. Grey vector proportionately indicates one body weight. **c**, Comparison of the alligator (left) and pigeon (right) right scapulocoracoids in lateral view, showing the saddle-shaped glenoid cartilages (blue) and homologous coracohumeral and acrocoracohumeral ligaments (white, cut at humeral attachment). Scale bars equal 1 cm.

AHL orientation intermediate between that in crocodylians (Fig. 3a) and extant birds (Fig. 3f).

An intermediate condition is also found in the recently discovered *Jeholornis*²¹ and *Sapeornis*²², which diverged from the line to extant birds between *Archaeopteryx* and *Confuciusornis*²². Hence, we conclude that the common ancestor of *Jeholornis* and extant birds had likely developed an incipient stabilizing role of the AHL (Fig. 3). On the basis of coracoid morphology, full development of the ligament-based force balance traces back at least to the common ancestor of Enantiornithes and Aves²³.

The selective impetus for transforming the coracoid tuberosity into an acrocoracoid process has been associated with the functional modification of three muscles. Displacement of the acrocoracoid directly affected the lines of action of the coracobrachialis and biceps brachii (coracoid head) because, like the AHL, both originate from the process²⁰. In addition, enlargement of the tuberosity formed the trisosseal canal, creating a pulley that deflected the tendon of the supracoracoideus such that this muscle became the primary humeral elevator/supinator powering upstroke¹⁵. We now also recognize elevation and expansion of the acrocoracoid process as directly related to the reorientation and increased loading of the AHL, which underlies the novel osseo-ligamentous mechanism for passive shoulder stabilization in modern birds.

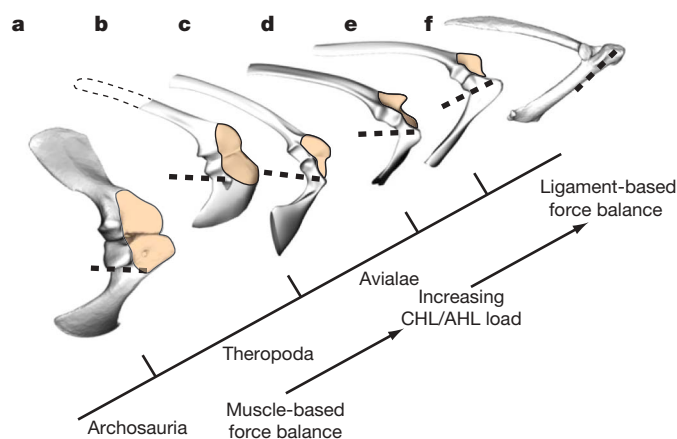


Figure 3 | Comparison of archosaur scapulocoracoids. Lateral view of right scapulocoracoids of *Alligator mississippiensis* (**a**), *Sinornithoides youngi* (**b**), *Sinornithosaurus millenii* (**c**), *Archaeopteryx lithographica* (**d**), *Confuciusornis sanctus* (**e**) and *Columba livia* (**f**) on a simplified phylogeny²³. The changing orientation of the CHL/AHL (dashed lines) and the reduction of the scapulocoracoid plate anterior to the glenoid for muscle attachment (orange surfaces) record the transition to a novel, ligament-based force balance mechanism in modern birds. The dashed lines do not represent ligament length.

METHODS

Pigeon model. Bones of a wild-caught pigeon (*Columba livia*) were scanned at the High-Resolution X-ray Computed Tomography Facility at the University of Texas at Austin (UTCT). Three-dimensional polygonal models were created using VTK (Kitware), articulated into a virtual skeleton in Maya (Autodesk), and configured in a mid-downstroke posture (humeral shaft protracted 60° from the vertebral axis, elevated 0° and pronated 15° relative to a neutral position with distal condyles vertical). On the basis of dissections, muscular and ligamentous attachments were mapped onto the virtual skeleton to determine their positions and lines of action (Fig. 1).

Three-dimensional force balance. The wing was treated as a free rigid body articulating only at the shoulder (elbow and wrist joints fixed). Aerodynamic, gravitational, muscular, joint and ligament forces were mapped onto the virtual skeleton as 16 vectors in Maya. These 3D vectors were used to calculate three translational components (F_x , F_y , F_z) and three rotational moments (M_x , M_y , M_z) relative to the coordinate system's origin at the point of glenohumeral contact (Fig. 2). Two vectors are fully described. A net aerodynamic force (F_a) of 0.5BW acts vertically upward at the centre of pressure, which was estimated to be 13.2 cm lateral and 1.1 cm posterior to the origin by averaging the quarter-chord points of ten chord-wise strips of equal area along the wing's 29.3 cm shoulder-wingtip span¹³. The wing's weight of 0.074BW acts vertically downward at its centre of mass (3.2 cm lateral and 0.8 cm posterior to the origin, based on a frozen, outstretched wing). All other vectors are only partially characterized. Muscle and ligament lines of action are fixed by anatomy and wing posture in all but the pectoralis, for which a range of vector directions were tested owing to its broad origin. Likewise, joint contact force orientation is constrained to horizontal by glenoid morphology. Maximum isometric muscle force (F_{max}) was estimated from the physiological cross sectional area of one pigeon and from published data^{24–26} (Table 1). However, the actual magnitudes of muscle, joint and ligament forces are unknown, creating an indeterminate system for which multiple answers exist.

A family of potential solutions was explored by interactively solving the 3D force balance using a MEL (Maya embedded language)-based expression to identify equilibrium. We discovered viable combinations of muscle activation using a simple workflow. All muscle forces began completely inactive (0BW), but could be increased up to F_{max} . First, a pectoralis force (F_p) was added to balance the aerodynamic elevation moment (wing weight was included but was not significant). Second, horizontal forces created by the pectoralis were balanced by the joint force (F_j). Third, the pectoralis's vertical force was countered—primarily by the ligament force (F_{ahl}) because muscles alone proved insufficient. Other muscles were then interactively recruited to balance remaining forces and moments, automatically adjusting previously entered F_p , F_j and F_{ahl} values as required. We sought simple alternatives that did not invoke unnecessary and widespread co-contraction (Fig. 2a, b; Table 1). The necessity for high AHL loading was insensitive to variation in pectoralis orientation or wing posture.

Mechanical testing. The coracoid–AHL–humerus complex was dissected from frozen pigeon specimens, each bone potted in low melting-temperature metal alloy and then mounted on an Instron Mechanical Testing System (Model #4442) with a 500 N load cell. Tensile force was measured for 15 loading/unloading cycles from 0–70 N (5 ligaments from 3 birds), followed by failure tests (10 ligaments from 6 birds). Crosshead speeds (rate of loading) ranged between 25–1000 mm min⁻¹, with data collected at either 6.67 or 20 points s⁻¹. The ligament substance was not completely torn in any of the failure tests. Failure occurred by humeral (6) or acroracoid (4) fracture.

Alligator shoulder data. Three alligators (1.08–3.08 kg) were recorded at 30 frames per second with simultaneous light (Sony DCR-TRV30) and dorso-ventral fluoroscopic video (Sony DCR-VX1000 digital handycam attached to a 27.94 cm image intensifier with a Siemens cineradiographic apparatus) as they walked on a motorized treadmill. Optical and radiographic distortions were removed by ‘warping’ images of square calibration grids in Maya. Shoulder and forelimb bone models were created using a 3D laser scanner (ShapeGrabber), articulated, and animated in Maya by aligning each bone to its fluoroscopic image²⁷. Shoulder kinematic data during walking were compared with ligament-taut positions derived by matching models to digital photographs of manipulated specimens.

Fossil reconstructions. Three-dimensional models of the scapula, coracoid and humerus were created in Maya based on measurements, photographs and drawings of the original material as well as published descriptions^{14,20,28–30}. The vertebral column, sternum, furcula and ribs (when present) were used to constrain the position and orientation of the scapulocoracoids. The thoracic vertebral column was oriented horizontally, with the humerus in a position comparable to that of the gliding pigeon model.

Received 21 July; accepted 10 November 2006.

Published online 17 December 2006.

- Hedrick, T. L., Usherwood, J. R. & Biewener, A. A. Wing inertia and whole-body accelerations: an analysis of instantaneous aerodynamic force production in cockatiels (*Nymphicus hollandicus*) flying across a range of speeds. *J. Exp. Biol.* **207**, 1689–1702 (2004).
- Spedding, G. R., Rosén, M. & Hedenström, A. R. A family of vortex wakes generated by a thrush nightingale in free flight in a wind tunnel over its entire natural range of flight speeds. *J. Exp. Biol.* **206**, 2313–2344 (2003).
- Biewener, A. A. & Dial, K. P. *In vivo* strain in the humerus of pigeons (*Columba livia*) during flight. *J. Morphol.* **255**, 61–75 (1995).
- Jenkins, F. A., Dial, K. P. & Goslow, G. E. J. A cineradiographic analysis of bird flight: the wishbone in starlings is a spring. *Science* **241**, 1495–1498 (1988).
- Goslow, G. E. J., Wilson, D. & Poore, S. O. Neuromuscular correlates to the evolution of flapping flight in birds. *Brain Behav. Evol.* **55**, 85–99 (2000).
- Tobalske, B. W. Neuromuscular control and kinematics of intermittent flight in the European starling (*Sturnus vulgaris*). *J. Exp. Biol.* **198**, 1259–1273 (1995).
- Tobalske, B. W., Peacock, W. L. & Dial, K. P. Kinematics of flap-bounding flight in the zebra finch over a wide range of speeds. *J. Exp. Biol.* **202**, 1725–1739 (1999).
- Chiappe, L. M. & Witmer, L. M. *Mesozoic Birds* (Univ. California Press, Berkeley, 2002).
- Dial, K. P. Wing-assisted incline running and the evolution of flight. *Science* **299**, 402–404 (2003).
- Xu, X. *et al.* Four-winged dinosaur from China. *Nature* **421**, 335–340 (2003).
- Gatesy, S. M. & Baier, D. B. The origin of the avian flight stroke: a kinematic and kinetic perspective. *Paleobiology* **31**, 382–399 (2005).
- Gray, S. J. *Animal Locomotion*. (Weidenfeld and Nicolson, London, 1968).
- Pennycuik, C. J. The strength of the pigeon's wing bones in relation to their function. *J. Exp. Biol.* **46**, 219–233 (1967).
- Jenkins, F. A. The evolution of the avian shoulder joint. *Am. J. Sci.* **293**, 253–267 (1993).
- Poore, S. O., Sánchez-Haiman, A. & Goslow, G. E. J. Wing upstroke and the evolution of flapping flight. *Nature* **387**, 798–802 (1997).
- Sy, M. Funktionell-anatomische untersuchungen am vogelflügel. *J. Ornithol.* **84**, 199–296 (1936).
- Bannasch, R. Morphologisch-funktionelle untersuchung am lokomotionsapparat der pinguine als grundlage für ein allgemeines bewegungsmodell des unterwasserfluges. *Gegenbaurs Morphol. Jahrb.* **132**, 757–817 (1986).
- Usherwood, J. R., Hedrick, T. L., McGowan, C. P. & Biewener, A. A. Dynamic pressure maps for wings and tails of pigeons in slow, flapping flight, and their energetic implications. *J. Exp. Biol.* **208**, 355–369 (2005).
- Jenkins, F. A. & Goslow, G. E. J. The functional anatomy of the shoulder of the Savannah monitor lizard (*Varanus exanthematicus*). *J. Morphol.* **175**, 195–216 (1983).
- Ostrom, J. H. Some hypothetical stages in the evolution of avian flight. *Smithson. Contrib. Paleobiol.* **27**, 1–21 (1976).
- Zhou, Z. & Zhang, F. A long-tailed, seed-eating bird from the Early Cretaceous of China. *Nature* **418**, 405–409 (2002).
- Zhou, Z. & Zhang, F. Anatomy of the primitive bird *Sapeornis chaoyangensis* from the early cretaceous of Liaoning, China. *Can. J. Earth Sci.* **40**, 731–747 (2003).
- Norell, M. A. & Clarke, J. A. Fossil that fills a critical gap in avian evolution. *Nature* **409**, 181–184 (2001).
- Dial, K. P. & Biewener, A. A. Pectoralis muscle force and power output during different modes of flight in pigeons (*Columba livia*). *J. Exp. Biol.* **176**, 31–54 (1993).
- Poore, S. O., Ashcroft, A., Sánchez-Haiman, A. & Goslow, G. E. J. The contractile properties of the M. supracoracoideus in the pigeon and starling: a case for long-axis rotation of the humerus. *J. Exp. Biol.* **200**, 2987–3002 (1997).
- Woolley, J. D. The functional morphology of the avian flight muscle M. coracobrachialis posterior. *J. Exp. Biol.* **203**, 1767–1776 (2000).
- Gatesy, S. M., Dial, K. P. & Jenkins, F. A. An inside look at skeletal motion in flying birds. *J. Vert. Paleo.* **24**, 63A (2004).
- De Beer, G. *Archaeopteryx lithographica: A Study Based upon the British Museum Specimen* (The Trustees of the British Museum, London, 1954).
- Paul, G. S. *Dinosaurs of the Air* (The Johns Hopkins University Press, Baltimore, 2002).
- Chiappe, L. M., Ji, S., Ji, Q. & Norell, M. A. Anatomy and systematics of the Confuciusornithidae (Theropoda: Aves) from the Late Mesozoic of Northeastern China. *Bull. Am. Mus. Nat. Hist.* **242**, 1–89 (1999).

Acknowledgements We are grateful to K. Dial for the pigeon specimen, K. Middleton for help with VTK, C. Sullivan and L. Claessens for sharing alligator video and specimens, Z. Zhou for access to fossils at IVPP, T. Roberts for methodological advice, and the Brown Morphology group. We thank Autodesk for Maya software support and the SHAPE lab at Brown University for access to 3D laser scanning equipment. Funding was provided by the National Science Foundation (S.M.G., SHAPE lab), a Bushnell Faculty Research Grant (S.M.G.), the Paleontological Society (D.B.B.) and Sigma Xi (D.B.B.).

Author Information Reprints and permissions information is available at www.nature.com/reprints. The authors declare no competing financial interests. Correspondence and requests for materials should be addressed to D.B.B. (David_Baier@brown.edu).